HHS Public Access

Author manuscript

Oncogene. Author manuscript; available in PMC 2012 September 15.

Published in final edited form as:

Oncogene. 2012 March 15; 31(11): 1342–1353. doi:10.1038/onc.2011.343.

MDM2 regulates MYCN mRNA stabilization and translation in human neuroblastoma cells

Lubing Gu[*], **Hailong Zhang**[*], **Jing He**, **Jiansha Li**, **Mei Huang**, and **Muxiang Zhou**

Department of Pediatrics, Aflac Cancer Center and Blood Disorders Service, Emory University School of Medicine, Atlanta, GA 30322

Abstract

The MYCN gene plays a critical role in determining the clinical behavior of neuroblastoma. Although it is known that genomic amplification occurs in high-risk subsets, it remains unclear how MYCN expression is regulated in the pathogenesis of neuroblastomas. Herein, we report that MYCN expression was regulated by the oncoprotein MDM2 at the post-transcriptional level and was associated with neuroblastoma cell growth. Increasing MDM2 by ectopic overexpression in the cytoplasm enhanced both mRNA and protein expression of MYCN. Mechanistic studies found that the C-terminal RING domain of the MDM2 protein bound to the MYCN mRNA's AU-rich elements within the 3′-untranslated region (3′UTR) and increased MYCN 3′UTR-mediated mRNA stability and translation. Conversely, MDM2 silencing by specific siRNA rendered the MYCN mRNA unstable and reduced the abundance of MYCN protein in MYCN-amplified neuroblastoma cell lines. Importantly, this MDM2 silencing resulted in a remarkable inhibition of neuroblastoma cell growth and induction of cell death through a p53-independent pathway. Our results indicate that MDM2 plays a p53-independent role in the regulation of both MYCN mRNA stabilization and its translation, suggesting that MDM2-mediated MYCN expression is one mechanism associated with growth of MYCN-associated neuroblastoma and disease progression.

Introduction

Neuroblastoma, the most common extracranial solid tumor seen in children, is a cancer of the peripheral nervous system. The hallmark of neuroblastoma is variability in clinical outcome: Some tumors regress spontaneously; whereas others will progress relentlessly, despite the most intensive treatment. An important factor that predicts a poor prognosis is the amplification of the MYCN gene, which occurs in about 25% of primary tumors. This amplification is strongly correlated with advanced-stage disease and treatment failure (Brodeur et al., 1984; Seeger et al., 1985).

Communications to: Muxiang Zhou, M.D. Division of Pediatric Hematology/Oncology Emory University School of Medicine 2015 Uppergate Drive Atlanta, GA 30322 U.S.A. Telephone: 404-727-1426 Fax: 404-727-4455 mzhou@emory.edu.

*These authors contributed equally to this work

Conflict of Interest The authors declare no conflicts of interest.

Like other members of the Myc family, the MYCN is a transcriptional regulator that appears to play a critical role in the control of diverse aspects of cellular physiology, including cell proliferation and apoptosis. MYCN has oncogenic potential, as studies demonstrate MYCN co-operates to transform primary cells, converts established cell lines to exhibit tumorigenicity, and initiates tumorigenesis in genetically-engineered mice (Weiss et al., 1997). Increased expression of MYCN correlates directly with the growth potential of neuroblastoma cells (Schweigerer et al., 1990; Negroni et al., 1991). Also, it has long been assumed that the malignant properties of MYCN are attributable to the deregulation of its expression, resulting in unencumbered cell proliferation (Hogarty, 2003).

It has been demonstrated that the expression of MYCN is not absolutely associated with the copy numbers of the gene that become amplified in children with neuroblastoma (Matthay, 2000); Tang et al., 2006). This suggested that the aggressive phenotype of MYCN seen in neuroblastoma might not only depend on MYCN itself, but also on other cellular signals that regulate MYCN expression. For example, the stability of MYCN mRNA is regulated by the AU-rich elements (ARE) within its 3′UTR, which provide signals for rapid degradation of the mRNA (Chen and Shyu 1995). HuD, a neuronal-specific RNA-binding protein, has been shown to bind to the ARE of the MYCN 3′UTR and stabilizes MYCN mRNA, thereby enhancing its expression (Lazarova et al., 1999; Manohar et al., 2002).

The human MDM2 gene is an oncogene that is also amplified in a variety of human cancers, including neuroblastoma (Corvi et al., 1995). High levels of MDM2 expression can occur in those neuroblastomas without MDM2 gene amplification, which is associated with a single nucleotide polymorphism in the MDM2 gene promoter in some cases (Cattelani et al., 2008). Additionally, it was reported that the expression of MDM2 can be transcriptionally induced by MYCN (Slack et al., 2005).

MDM2 gained considerable attention following its identification as the protein that negatively regulates the tumor suppressor p53 (Momand et al., 1992; Haupt et al., 1997). MDM2 also plays p53-independent roles in oncogenesis. Increasing evidence suggests that even in cancer patients having p53 deficiencies, overexpression of MDM2 is still involved in the promotion of cancer, resistance to treatment and progression of disease (Jones et al., 1998; Zhang and Zhang, 2005). Therefore, in addition to interacting with and regulating p53, MDM2 appears to interact with other molecules involved in oncogenesis. For instance, MDM2 has the capacity to bind to some RNA molecules (Elenbaas et al., 1996; Lai et al., 1998; Poyurovsky et al., 2003; Anderson et al., 2007; Candeias et al., 2008). More specifically, binding of the C-terminal RING domain of the MDM2 protein to the XIAP mRNA does regulate translation of this important apoptosis regulator, which is involved in the development of resistance to anticancer treatment (Gu et al., 2009).

Our laboratory was prompted to investigate MDM2’s regulation of MYCN by a fortuitous finding during an investigational approach to knockdown MDM2 as a potential treatment for neuroblastoma, in which we found that the silencing of MDM2 resulted in a reduction of MYCN expression and an inhibition of cell growth, in MYCN-amplified neuroblastoma. The possible regulation of MYCN by MDM2 and the mechanism by which MDM2 induces MYCN expression in neuroblastoma were investigated in the current study.

Results

Modification of MDM2 is associated with altered expression of MYCN

To evaluate whether there is an association between modification of MDM2 and exchanges of MYCN expression, we first tested the effect of MDM2 silencing on MYCN expression in two MDM2-overexpressing/MYCN-amplified cell lines, LA1-55N (p53-null) and NB-1691 (p53-wt). We found that a stable transfection of siMDM2 in LA1-55N cells significantly inhibited the endogenous MDM2 expression. Transfection of the siMDM2 containing a single-nt mutation in the 19-nt MDM2 sequence, siMDM2 (m), largely diminished the previously observed inhibitory effect on MDM2 (Fig. 1A). We failed to obtain clones in the stable transfection of siMDM2 (wt) in NB-1691 cells that express very high levels of MDM2 and have a wt-p53 phenotype, due to no cell growth in the transfection. Therefore, we performed a transient transfection of the siMDM2 (wt) and siMDM2 (m), respectively, into NB-1691 cells. We found that the expression of MDM2 was similarly inhibited by these plasmids, as in the LA1-55N cells (Fig. 1B). Interestingly, we found a concomitant and corresponding reduction of MYCN expression in the two MYCN-amplified neuroblastoma cell lines that were either stably or transiently transfected with siMDM2 plasmids (Fig. 1A and B). However, the ectopic MYCN that was transfected in the non-MYCN amplified SHEP-Tet/21N cells was not inhibited by knockdown of MDM2 with siMDM2 (Fig. 1C).

Next, we performed MDM2 gene transfection in a non-MYCN amplified neuroblastoma cell line SK-N-SH that express very low level of MDM2 and MYCN, to see whether enforced overexpression of MDM2 has a role in stimulating MYCN expression. The wt-MDM2 as well as MDM2 mutations at 166 (MDM2/166A that cannot be phosphorylated, and MDM2/166E that mimics phosphorylated MDM2) (Mayo and Donner, 2001) were used for transfection. Similar to our previous studies (Gu et al., 2009), transfection of MDM2/166A plasmid tagged by red fluorescence protein (pDsRed1-C1) showed that MDM2/166A was predominantly expressed in the cytoplasm, whereas MDM2/166E was mainly localized in the nucleus (Fig. 1D). Transfection of MDM2/166A in SK-N-SH cells significantly upregulated MYCN protein expression. In contrast, transfection of MDM2/166E did not obviously upregulate MYCN as compared to the transfection of MDM2/166A and wt-MDM2 (Fig. 1E); suggesting that it is the cytoplasmic, but not nuclear MDM2 that can induce MYCN expression.

MDM2 regulates MYCN mRNA stabilization

We evaluated the molecular mechanism by which the cytoplasmic MDM2 induces MYCN expression. We began by testing the effect of cytoplasmic MDM2 on MYCN mRNA expression. RT-PCR results showed that inhibition of MDM2 by siRNA downregulated MYCN mRNA expression in a dose-dependent manner in the NB-1691 cells that express high levels of MDM2 and MYCN (Fig. 2A and B). In addition, transfection of the MDM2/166A plasmid into SK-N-SH cells induced MYCN mRNA expression (Fig. 2A). Then we examined the effect of MDM2 on MYCN mRNA stabilization. We performed both Northern blot assay and quantitative RT-PCR to elucidate MYCN mRNA turnover after treatment with actinomycin D to inhibit mRNA synthesis, in NB-1691 cells that were transfected with MDM2 siRNA and in SK-N-SH cells that were transfected with

MDM2/166A. As shown in Fig. 2C, Northern blot results indicated that inhibition of MDM2 in high MDM2-producing cells by siRNA significantly reduced the stability of the MYCN mRNA. In contrast, the half-life of MYCN mRNA in SK-N-SH cells was increased by transfection of the MDM2/166A plasmid (Fig. 2D).

MDM2 does not regulate MYCN transcription, IRES-dependent translation and post-translation

To evaluate whether MDM2 regulates MYCN transcription, we cloned the MYCN gene promoter as described (Sivak et al., 1997; Horvilleur et al., 2008) into the pGL3-basic vector and performed a gene transfection and reporter assay. Co-transfection of either wt-MDM2 or MDM2/166A plasmids did not stimulate the MYCN promoter-mediated luciferase activity (Fig. 3A), suggesting that MDM2 did not regulate MYCN gene transcription. As a control, p73α increased the promoter activity (Horvilleur et al., 2008). Additionally, we constructed a dicistronic *Renilla* luciferase (RL) and *firefly* luciferase (FL) plasmid in pRL-FL, containing the MYCN 5′-UTR IRES (pRL-MYCN 5′UTR-FL). We performed a similar transfection and reporter assay with the pRL-MYCN 5′UTR-FL plasmid in SK-N-SH cells, and found that MDM2 did not affect MYCN IRES activity (Fig. 3B). Consistent with previous report by Cobbold et al (Cobbold et al., 2008), the MYCN IRES-binding protein YB-1 stimulated MYCN IRES activity. Furthermore, we performed pulse-chase experiments using CHX to evaluate whether the observed reduced MYCN expression in the MDM2-silenced cells may also involve a post-translational mechanism. As shown in Fig. 3C, the half-life of the MYCN protein in MDM2 siRNA-transfected cells did not change, as compared with that of control cells. These results suggest that the observed MDM2-upregulated expression of MYCN most likely occurred at the translational level, through stabilization of MYCN mRNA.

The C-terminal RING domain of the MDM2 protein binds to the 3′UTR of MYCN mRNA

We investigated whether MDM2 can stabilize MYCN mRNA through binding to the 3′UTR of MYCN. First, we performed a protein-RNA binding assay to search for a possible association *in vivo* between the MDM2 protein and MYCN mRNA. Results from IP and RT-PCR showed that the MDM2 protein, like HuD, was able to bind MYCN mRNA (Fig. 4A). To investigate whether MDM2 binds specifically to the MYCN 3′UTR, we performed UV cross-linking of a ^{32}P-labeled MYCN 3′UTR probe with cell extracts from MDM2/166A-transfected SK-N-SH cells that were immunoprecipitated with MDM2 and HuD antibodies. The MYCN 5′UTR IRES that was labeled with ^{32}P served as a control. We found that both MDM2 and HuD were able to bind to the MYCN 3′UTR probe, but not to the MYCN 5′UTR IRES element (Fig. 4B).

To further confirm that the MDM2 protein binds to the MYCN 3′UTR, we performed UV cross-linking and gel electrophoresis with a recombinant human MDM2 (rhMDM2) and a ^{32}P-labeled MYCN 3′UTR probe. Results showed that the MDM2 protein strongly and specifically bound to the MYCN 3′UTR RNA *in vitro*, without other cellular elements present (Fig. 4C). The non-related recombinant protein Bcl-2 did not bind to the MYCN 3′UTR RNA. In addition, we performed similar UV cross-linking and gel electrophoresis to screen for the domain of MDM2 required for its binding to the MYCN 3′UTR. RNA binding

assays revealed that the C-terminal RING domain (425-491), but not other parts of the MDM2 protein (1-424), was able to bind to the MYCN 3′UTR (Fig. 4D). The binding of fragment (434-491) to the MYCN 3′UTR was not detected, suggesting that the 10 amino acids from 425-434 are critical for the binding. Consistent with the *in vivo* protein-RNA binding assay, the GST-fused HuD strongly bound to the MYCN 3′UTR RNA probe.

To rule out the possibility that MDM2 binds to the MYCN 3′UTR through its interaction with HuD, we tested for any physical binding between the MDM2 and HuD proteins. Immunoprecipitation and Western blot assay results showed that MDM2 did not interact with HuD (Fig. 4E).

MDM2 regulates MYCN translation

Since MDM2 stabilized MYCN mRNA, we evaluated whether MYCN protein synthesis is enhanced by MDM2. We performed linear sucrose gradient fractionation to assess the association between polyribosomes and the MYCN mRNA in SK-N-SH cells that were transfected with the MDM2/166A plasmid and the control plasmid (Fig. 5A). We found that MYCN mRNA in MDM2/166A-transfected cells was clearly shifted from fractions containing translation-dormant complexes (Fig. 5B, fractions 1-4) to fractions that were enriched with translating polyribosomes (Fig. 5B, fractions 5-11), which is indicative of enhanced translation. This observation was likely specific, because MDM2/166A expression had no effect on the polyribosome profile of a control GAPDH mRNA. Thus, induction of MYCN expression by MDM2 appeared to occur at the translational level.

Next, we performed gene transfection and reporter assay to confirm that MDM2 induces MYCN translation and to ascertain whether the translational effect is exerted through the 3′UTR. We constructed a FL reporter plasmid in a pGL3-promoter containing the MYCN 3′UTR (pGL3-MYCN 3′UTR). Various control plasmids, such as the MYCN 3′UTR with ARE mutations and with antisense orientation were also constructed. These were transiently transfected into SK-N-SH cells together with the MDM2/166A and HuD plasmids, or into NB-1691 cells together with the siMDM2 and siHuD plasmids. Co-transfection of the MDM2 and HuD expression plasmids similarly increased the FL activity in SK-N-SH cells transfected with the pGL3-MYCN 3′UTR plasmid (Fig. 5C), but did not in the same cells transfected with the pGL3-MYCN 3′UTR plasmid with the ARE mutation in the 3′UTR. In contrast, knockdown of MDM2 and HuD by siRNA reduced the FL activity in NB-1691 cells transfected with the pGL3-MYCN 3′UTR in a sense, but not antisense, orientation (Fig. 5D). Collectively, these results indicated that MDM2 regulates MYCN translation through stabilization of the 3′UTR of MYCN mRNA.

MDM2-mediated MYCN expression is p53-independent

To evaluate whether the MDM2-mediated MYCN expression is associated with p53 or p73, we examined the expression of p53 in NB-1691 (wt-p53) and p73 in LA1-55N (p53-null), respectively. Surprisingly, the expression of p53 and its targets p21 and PUMA for regulation of cell cycle arrest and apoptosis in NB-1691 cells was not increased by transfection of siMDM2 (Fig. 6A). Also, the expression of p73 in LA1-55N was not activated by inhibition of MDM2 (Fig. 6B). In addition, we tested the regulation of p53 as

well as MYCN in siMDM2 treated SHEP-Tet/21N line with overexpression of MDM2 and with conditional expression of ectopic MYCN that was not regulated by MDM2 (Fig. 1C) due to lack of original 3′UTR. We found that the expression of p53 was induced by siMDM2 in both SHEP-Tet/21N in the presence of tetracycline (without MYCN expression) and SHEP-Tet/21N in the absence of tetracycline (with MYCN expression) (Fig. 6C). The induction of p53 was not accompanied by any changes of MYCN expression in these lines, suggesting that MDM2-mediated MYCN 3′-UTR stability and MYCN protein synthesis is p53-independent. Furthermore, we performed assays either to inhibit p53 using siRNA or to induce p53 with the MDM2-p53 inhibitor nutlin-3 in NB-1691 cells to evaluate the possible effect of p53 on MDM2-regulation of MYCN. Inhibition of p53 by siRNA resulted in slightly decrease in expression of both MDM2 and MYCN (Fig. 6D). Blockade of MDM2-p53 interaction by nutlin-3 led to stabilization of p53 and increase in MDM2 expression (Fig. 6E). However, the expression of MYCN was not obviously increased following enhanced MDM2 expression in nutlin-3 treated cells. These suggest that MYCN is regulated neither by p53 nor by nuclear MDM2 that is transcriptionally induced by stabilized p53 following treatment of the non-stressing agent nutlin-3.

MDM2-mediated MYCN expression regulates neuroblastoma cell growth

Next, we evaluated the effect of MDM2-regulation of MYCN on cell growth in neuroblastoma. By clonogenic assay for NB-1691 cells that were transfected with the siMDM2, we found that the persistent expression of siMDM2 in NB-1691 cells completely inhibited colony formation (Fig. 7A). Colonies can be formed by the cells with a persistent expression of the siMDM2 (m), but the numbers of colonies were reduced when compared with cells that were transfected with the control siRNA. Because, the expression and function of p53 was not activated in NB-1691 (Fig. 6A), this suggests that downregulation of MYCN by knockdown of MDM2 play a critical role in growth inhibition of MYCN-amplified neuroblastoma. In contrast, we evaluated the possibly opposite impact of enforced overexpression of MDM2 on MYCN-mediated cell growth. Enforced cytoplasmic expression of MDM2 in SK-N-SH cells remarkably (2.5-3.5 folds) increased the colony formation of these cells (Fig. 7B). To confirm the role of upregulated MYCN following increased MDM2 expression in cell growth, we also tested for colony formation of those same MDM2/166A-transfected SK-N-SH cells, but in the presence of siMYCN. The siMYCN but not control siRNA treatment inhibited the previously-observed colony formation of MDM2/166A-transfected SK-N-SH cells. As control, siMYCN did not inhibit growth of SK-N-SH cells that were not transfected with MDM2/166A, suggesting that MDM2/166A-upregulated MYCN confers increased cell proliferation and growth.

In addition, we compared the effect of siMDM2 on growth of SHEP-Tet/21N line in the presence and absence of MYCN to further validate the critical role of MDM2-mediated regulation of MYCN in neuroblastoma growth. Clonogenic assay results showed that siMDM2-mediated inhibition of colony formation was significantly reduced in MYCN expressed SHEP-Tet/21N as compared in non-MYCN expressed SHEP-Tet/21N (Fig. 7C), although the levels of basic p53 expression and induction by siMDM2 in the former was even higher than in the latter (Fig. 6C). This suggests that the ectopic MYCN, which is not inhibited by siMDM2, reverse the siMDM2-mediated growth inhibition.

Furthermore, we tested the effect of the siMDM2-mediated downregulation of MYCN on sensitivity of LA1-55N cells in response to ionizing radiation (IR) treatment. As shown in Fig. 7D, a flow-cytometric apoptosis assay showed that a significantly increased percentage of LA1-55N cells treated with IR plus siMDM2 were annexin-V positive at 48-h post-treatment as compared to IR plus siRNA control. Because LA1-55N cells lack p53 and induction of p73 following siMDM2 (Fig. 6B), we believe that the siMDM2-mediated downregulation of MYCN is critical for the increased sensitivity to IR treatment.

Discussion

There has been some prior indication in the literature that MDM2 plays a critical role in Myc-driven tumorigenesis. In a transgenic mouse model, haplo-deficiency of MDM2 profoundly inhibits C-Myc-induced lymphomagenesis (Alt et al., 2003) and MYCN-stimulated neuroblastoma tumorigenesis (Chen et al., 2009). These studies demonstrated that the suppression of Myc-mediated tumorigenesis by insufficiency of MDM2 was attributed to the activation of p53. In our neuroblastoma cell line model, knockdown of MDM2 by siRNA indeed remarkably inhibited cell growth of MYCN-amplified neuroblastoma having a wt-p53. We also found that silencing of MDM2 inhibited cell growth of MYCN-amplified neuroblastoma with a p53-null phenotype. Our results suggested that p53-independent signaling pathways are involved in MDM2-mediated tumor cell growth in MYCN-amplified neuroblastoma.

By examining the expression of MYCN in these neuroblastoma cells after siMDM2 transfection, we found that MYCN expression was concomitantly and proportionally reduced following siRNA-mediated inhibition of MDM2, suggesting that MDM2 may have a role in inducing MYCN expression. Enforced expression of MDM2 by gene transfection proved that MDM2 stimulates MYCN expression. Further mechanistic studies demonstrated that the C-terminal RING domain of MDM2 was able to bind to the ARE within the 3′UTR of MYCN mRNA and it stabilized the MYCN mRNA, resulting in enhanced MYCN protein synthesis.

Post-transcriptional control of MYCN is well documented. The 3′UTR of MYCN contains two typical ARE (AUUUA) repeats that mediate mRNA instability (Lazarova et al., 1999). HuD binds to these AREs and increases the stability of the MYCN mRNA and thus, protein synthesis (Manohar et al., 2002; Wang et al., 2001). In the present study, our results showed that MDM2 is similar to HuD, as it also regulated MYCN mRNA stabilization. However, unlike HuD that is uniformly and highly expressed in N-type neuroblastoma cells but not substrate-adherent (S)-type neuroblastoma cells (Ross et al., 1997), MDM2 can be expressed in both N and S cells. Furthermore, the expression levels of HuD in cultured cells are always associated with the levels of MYCN expression (Lazarova et al., 1999). However, in our 7 neuroblastoma cell lines studied, there was no coincidence of expression between MDM2 and MYCN in growing cells (data not shown). Our possible explanation for the discrepancy between MYCN and MDM2 expression in cultured cells, in comparison to the solid association seen with HuD, was based on the premise that there was likely a dependence on the different subcellular distribution of HuD and MDM2 proteins in growing cells. The HuD protein is mostly expressed in the cytoplasm (Fornaro et al., 2007), whereas MDM2 is a

nuclear phosphoprotein. The cytoplasmic HuD could persistently stabilize MYCN mRNA in the cytoplasm, resulting in direct increases in MYCN protein synthesis. Therefore, high levels of HuD expression will always be accompanied by increased MYCN expression in cultured cells. In contrast, in cultured, growing cells, MDM2 is phosphorylated and exclusively localized in the nucleus, where it would be unable to regulate MYCN mRNA stability. This concept was ascertained by the results of our experiments using nutlin-3 treatment, where transcriptionally increased MDM2 in the nucleus following nutlin-3-stabilized p53 was unable to induce MYCN expression. Under conditions when the MDM2 protein is translocated from the nucleus to the cytoplasm, it can bind to the MYCN mRNA and regulate its stability and translation. This notion was also ascertained by the results of our experiments using gene transfection of a mutant MDM2 (at site 166), where it was found that cytoplasmic, but not nuclear MDM2 stimulated MYCN expression.

In our previous studies, we characterized the ability of MDM2 to bind cellular RNA. We demonstrated that the cytoplasmic, but not the nuclear MDM2 protein, binds to the XIAP IRES mRNA and induces XIAP translation (Gu et al., 2009). In the current study, we tested the binding capacity of MDM2 to the MYCN IRES and found that MDM2 did not bind to it, nor induce IRES-dependent translation of MYCN. By analyzing and comparing the RNA sequences in XIAP IRES and MYCN IRES, we found the XIAP IRES contains multiple AU-rich sequences, whereas the MYCN IRES does not. This suggested that the AU-rich RNA sequence is essential for the MDM2 interaction and subsequent regulation to occur. Furthermore, by protein mapping analysis, we found that consistent with MDM2's binding to other RNA molecules such as p53 and XIAP mRNA (Candeias et al., 2008; Gu et al., 2009), it is the C-terminal RING domain, not other parts of the protein, that bound to the 3′UTR of MYCN RNA.

It is well documented that MDM2 plays a role in MYCN-mediated tumor growth and is a predictor for poor treatment outcome in neuroblastoma patients (Cattelani et al., 2008; Chen et al., 2009). Because MDM2 is known as an important inhibitor of the tumor suppressor p53, there is no doubt about the critical p53-dependent role MDM2 plays in neuroblastoma tumorigenesis and disease progression. However, in our cell model, the p53 function was not activated by knockdown of MDM2 in neuroblastoma that has overexpression of both MDM2 and MYCN. Our explanation for this is that because p53 is a direct transcriptional target of MYCN (Chen et al., 2010), any MDM2 inhibition-mediated increases in p53 expression became diminished or abrogated by the downregulation of MYCN that decreased p53 transcription in these MDM2/MYCN-overexpressing neuroblastoma cells. Our present study provided strong evidence to demonstrate that the MDM2-mediated MYCN expression is p53-independent, as indicated by that the alteration of MYCN expression was closely associated with the changes of MDM2 (in cytoplasm) but not with the fluctuation of p53 level. This p53-independent role of MDM2 in directly inducing MYCN expression is critical for neuroblastoma growth. Furthermore, it is of note that during cellular stress and DNA damage such as exposure to irradiation or chemotherapy, the MDM2 protein becomes dephosphorylated and thus translocates from the nucleus to the cytoplasm (Gu et al., 2009; Okamoto et al., 2002; Meek and Knippschild, 2003). This cytoplasmic MDM2 would stabilize MYCN mRNA and increase MYCN protein synthesis, which is likely an important mechanism involved in the development of radiochemotherapy resistance in MDM2-

overexpressing, MYCN-amplified neuroblastoma. Our results of experiments in studying the p53-null, MDM2/MYCN-overexpressing line LA1-55N suggested this possibility, where downregulation of MYCN by siMDM2 significantly increased sensitivity of LA1-55N cell to IR treatment.

Because of our comparison of growth in isogenic cells with and without MDM2 knockdown, we found that the silencing of MDM2 by siRNA remarkably inhibited MYCN expression and tumor cell growth in MYCN-amplified neuroblastoma. In particular, we discovered that the cell death of p53-deficient MYCN-amplified neuroblastoma cells induced by IR was enhanced after siRNA-mediated inhibition of the cell's MDM2. Thus, our present study provided an insight that means approaches directly targeting MDM2, rather than targeting the interaction between MDM2 and p53, would likely be a productive novel concept for the development of anticancer treatment of MYCN-amplified refractory neuroblastoma.

Materials and Methods

Cell lines

Four human neuroblastoma cell lines (NB-1691, LA1-55N, SK-N-SH and SHEP-Tet/21N) were used in this study. Two of the four neuroblastoma cell lines (NB-1691 and LA1-55N) had MYCN gene amplification and NB-1691 also had MDM2 gene amplified. Three of the four lines (NB-1691, SK-N-SH and SHEP-Tet/21N) were wild-type (wt) p53, while the LA1-55N cell line was p53-null as previously characterized (Thompson et al., 1997; Peirce et al., 2009; Carr et al., 2006). NB-1691, LA1-55N, SK-N-SH lines were obtained from Dr. H. Findley (Emory University), while the SHEP-Tet/21N with conditional MYCN expression was kindly provided by Dr. M. Schwab (dkfz, Germany).

Plasmids and gene transfection

The MDM2 expression plasmid pCMV-MDM2 was provided by Dr. B. Vogelstein (Johns Hopkins University). Also, the wt MDM2 cDNA was cloned into a pDsRed1-C1 vector, to generate the plasmid pDsRed1-C1/MDM2. The Quick Change site-directed mutagenesis kit was used to mutate the Akt phosphorylation site from serine 166 to either alanine or glutamic acid (MDM2/166A or MDM2/166E, respectively) in pCMV-MDM2 and pDsRed1-C1/MDM2. The HuD expression plasmid was generated by cloning the HuD cDNA into the pcDNA3.1 vector. The wt and various C-terminal truncated GST-tagged MDM2 and HuD constructs were generated by polymerase chain reaction and cloned into the bacterial pGEX expression vector. The pSUPER MDM2, HuD and MYCN siRNA plasmids were constructed by inserting specific 19 nucleotide (nt) MDM2, HuD and MYCN sequences into an expression plasmid, pSUPER-neo, respectively.

The pGL3-MYCN 3′UTR reporter plasmid was constructed by inserting a 862 base-pair (bp) segment of the MYCN 3′UTR into a pGL3-Promoter (pGL3P) plasmid. The sense and antisense orientations of the MYCN 3′UTR in the luciferase reporter were identified by both enzyme digestion and DNA sequencing. A pGL3-MYCN 3′UTR plasmid containing mutated ARE within the 3′UTR was constructed as a control. Detailed description of these

plasmids constructions and gene transfection and reporter analysis were seen in the supplemental data online.

Western blot analyses

Cell proteins were prepared by lysing cells for 30 min at 4° C in a lysis buffer composed of 150 mM NaCl, 50 mM Tris (pH 8.0), 5mM EDTA, 1% (v/v) Nonidet p-40, 1 mM phenylmethylsulfonyl fluoride (PMSF), 20 μg/ml aprotinin and 25 μg/ml leupeptin. Equal amounts of protein extracts were resolved by sodium dodecyl sulfate-polyacrylamide gel electrophoresis (SDS-PAGE) and transferred to a nitrocellulose filter. After blocking with buffer containing 5% non-fat milk, 20 mM Tris-HCl (pH 7.5), and 500 mM NaCl for 1 h at room temperature; the filter was incubated with specific antibodies for 1 h at room temperature; washed and followed by an incubation with HRP-labeled secondary antibody; and then developed using a chemiluminescent detection system (ECL, Amersham Life Science, Buckinghamshire, England).

Northern blot and mRNA degradation rate assay

For these assays, RNA synthesis was terminated by addition of 5 mg/ml actinomycin D. Cells were harvested at different time points after actinomycin D addition and total RNA was isolated. RNA was electrophoresed on a 1% agarose/6% formaldehyde gel and transferred to a nylon filter. Probes were prepared by a randomized-labeling approach using α-^{32}P-dCTP. Hybridization was performed in 50% (v/v) formamide/5× SSC/1% SDS/5× Denhardt's/20% dextran sulfate/100μg/ml sheared salmon sperm DNA solution, at a temperature of 42° C for 16 h. After a final wash in 1× SSC/0.1% SDS at 65° C for 30 min, the filter was autoradiographed. The amount of MYCN mRNA remaining was determined by densitometric analysis of the band in the Northern blot. Comparisons between experiments were carried out by normalizing the starting MYCN mRNA levels (defined as 1 unit).

Pulse-chase assay

The turnover of protein was tested by a standard protein-synthesis inhibitor cycloheximide (CHX) assay. Briefly, cells were treated with 50μg/ml CHX for different times before lysis in the presence of siMDM2 or siRNA control, and the expression of MYCN was detected by Western blot analysis.

Reverse transcription (RT)-PCR

The total RNA was extracted with the RNeasy Mini Kit (Qiagen, Hilden, Germany) to examine the expression of MYCN mRNA in MDM2-transfected or silenced cells. RT-PCR was performed with an Access RT-PCR Kit (Promega Corporation) according to the manufacturer's protocols. The resulting PCR products were run on a 1.5% agarose gel and visualized with ethidium bromide staining under UV light. For testing of MYCN mRNA expression in the polysom profiling experiments, first-strand cDNA synthesis was performed with a mixture of random nonamers and oligo-dT as primers (Qiagen). Amplification of MYCN was performed with a 7500 Real-Time RT-PCR System (Applied Biosystems, Foster City, CA), using a QuantiFast SYBR Green RT-PCR kit (Qiagen)

according to the manufacturer's instructions. The primers for MYCN and the house-keeper gene GAPDH were purchased from Qiagen.

Polysome preparation and analysis

Polysome profiling was carried out as described previously (Gu et al., 2009), with only slight modifications. Briefly, SK-N-SH cells transfected with MDM2-166A or with empty vector, as described in the corresponding experiments, were incubated with 100μg/ml cycloheximide (CHX) for 15 min in order to arrest polyribosome migration. To isolate cytoplasmic RNA, cells were lysed in a buffer containing 20mM Tris-HCl at pH 8.0, 100mM NaCl, 5 mM $MgCl_2$, 0.5% Triton X-100, 500U/ml RNAsin and a cocktail of protease inhibitors. Fractionation on a 15-45% (w/v) sucrose gradient followed, by centrifugation in a SW41Ti rotor at 39,000rpm for 1 hr. Fractions were collected from each gradient tube by upward replacement, with monitored absorption at OD_{254} using a fractionator (Isco, Lincoln, NE). The RNA in each fraction was extracted and subjected to RT-PCR, as described above.

Expression of GST-tagged proteins

The expression and purification of GST-fused MDM2 and HuD proteins were performed as described previously (Gu et al., 2009). Briefly, after transfection of various GST-fused MDM2 and HuD plasmids into BL21 *Escherichia coli*, the cells were incubated in LB medium at 30°C. After incubation with 0.1 mM IPTG for 2 h, the cells were harvested. GST-fused proteins were purified by lysing the induced cells with sonication, followed by isolation with glutathione-agarose beads (Pharmacia). The purity and correct expression of each of the GST-fused proteins were analyzed by gel electrophoresis and Coomassie G250 staining, as well as by western blot assay using anti-GST antibody.

UV cross-linking and RNA binding assays

UV cross-linking and immunoprecipitation assays were performed as described previously (Gu et al., 2009). Briefly, the DNA templates for synthesis of the MYCN 3′UTR RNA probe and the MYCN 5′UTR IRES RNA probe were generated by PCR using specific primer pairs. MYCN 3′UTR probe with mutations in ARE was also synthesized, as a control. Internally-labeled RNA probes were synthesized by *in vitro* transcription with T7 polymerase (MAXIScript T7 RNA polymerase kit, Ambion) in the presence of [α-^{32}P] UTP. The cell extracts or purified recombinant proteins were mixed with ^{32}P-labeled RNA probes. UV cross-linking of the RNA-protein complexes was performed and then resolved by 10% SDS-PAGE gel and visualized by autoradiography.

MYCN mRNA was co-immunoprecipitated with MDM2 antibody from whole-cell extracts by using the modified method, as described previously (Gu et al., 2009) to detect the *in vivo* binding of MDM2 protein and MYCN mRNA (see detailed description in the supplemental data online).

Clonogenic assay

The soft agarose method was used to measure colony formation. Briefly, a bottom layer of a low-melting-point agarose solution containing 0.5% agarose in a final concentration of 1X

RPMI 1640 medium supplemented with 10%FBS was poured into gridded 35 mm dishes and allowed to gel. A top layer contained the prepared cells, 0.35% agarose, and 1 X medium as the diluent. Cells were cultured at 37°C in a humidified atmosphere containing 5%CO_2. After 2 to 3 weeks, the cultures were fixed with formalin and the colonies formed were scored (using a cutoff value of 50 viable cells).

Apoptosis assays

An annexin-V assay (Oncogene, San Diego, CA) was used to quantitate apoptotic cells. Briefly, cells with or without a given treatment were washed once with PBS and then stained with FITC-annexin-V and PI for 30 min, according to the manufacturer's instructions. Stained cells were detected using the FACScan (Becton Dickinson) and analyzed using WinList software (Verity Software House Inc).

Supplementary Material

Refer to Web version on PubMed Central for supplementary material.

Acknowledgments

This work was supported by the National Institutes of Health (R01 CA123490, R01CA143107 to MZ) and CURE (MZ and LG).

References

Alt JR, Greiner TC, Cleveland JL, Eischen CM. Mdm2 haplo-insufficiency profoundly inhibits Myc-induced lymphomagenesis. EMBO J. 2003; 22:1442–1450. [PubMed: 12628936]

Anderson JJ, Challen C, Atkins H, Suaeyun R, Crosier S, Lunec J. MDM2 RNA binding is blocked by novel monoclonal antibody h-MDM2-F4-14. Int J Oncol. 2007; 31:545–555. [PubMed: 17671681]

Brodeur GM, Seeger RC, Schwab M, Varmus HE, Bishop JM. Amplification of N-myc in untreated human neuroblastomas correlates with advanced disease stage. Science. 1984; 224:1121–1124. [PubMed: 6719137]

Candeias MM, Malbert-Colas L, Powell DJ, Daskalogianni C, Maslon MM, Naski N, et al. P53 mRNA controls p53 activity by managing Mdm2 functions. Nat Cell Biol. 2008; 10:1098–1105. [PubMed: 19160491]

Carr J, Bell E, Pearson AD, Kees UR, Beris H, Lunec J, et al. Tweddle DA. Increased frequency of aberrations in the p53/MDM2/p14(ARF) pathway in neuroblastoma cell lines established at relapse. Cancer Res. 2006; 66:2138–2145. [PubMed: 16489014]

Cattelani S, Defferrari R, Marsilio S, Bussolari R, Candini O, Corradini F, et al. Impact of a single nucleotide polymorphism in the MDM2 gene on neuroblastoma development and aggressiveness: results of a pilot study on 239 patients. Clin Cancer Res. 2008; 14:3248–3253. [PubMed: 18519749]

Chen CY, Shyu AB. AU-rich elements: characterization and importance in mRNA degradation. Trends Biochem Sci. 1995; 20:465–470. [PubMed: 8578590]

Chen L, Iraci N, Gherardi S, Gamble LD, Wood KM, Perini G, et al. p53 is a direct transcriptional target of MYCN in neuroblastoma. Cancer Res. 2010; 70:1377–1388. 5. [PubMed: 20145147]

Chen Z, Lin Y, Barbieri E, Burlingame S, Hicks J, Ludwig A, et al. Mdm2 deficiency suppresses MYCN-driven neuroblastoma tumorigenesis in vivo. Neoplasia. 2009; 11:753–762. [PubMed: 19649205]

Cobbold LC, Spriggs KA, Haines SJ, Dobbyn HC, Hayes C, de Moor CH, et al. Identification of internal ribosome entry segment (IRES)-trans-acting factors for the Myc family of IRESs. Mol Cell Biol. 28:40–49. [PubMed: 17967896]

Corvi R, Savelyeva L, Breit S, Wenzel A, Handgretinger R, Barak J, et al. Non-syntenic amplification of MDM2 and MYCN in human neuroblastoma. Oncogene. 1995; 10:1081–1086. [PubMed: 7700632]

Elenbaas B, Dobbelstein M, Roth J, Shenk T, Levine AJ. The MDM2 oncoprotein binds specifically to RNA through its RING finger domain. Mol. Med. 1996; 2:439–451. [PubMed: 8827714]

Fornaro M, Raimondo S, Lee JM, Giacobini-Robecchi MG. Neuron-specific Hu proteins sub-cellular localization in primary sensory neurons. Ann Anat. 2007; 189:223–228. [PubMed: 17534028]

Gu L, Zhu N, Zhang H, Durden DL, Feng Y, Zhou M. Regulation of XIAP translation and induction by MDM2 following irradiation. Cancer Cel. 2009; 15:363–375.

Haupt Y, Maya R, Kazaz A, Oren M. Mdm2 promotes the rapid degradation of p53. Nature. 1997; 387:296–299. [PubMed: 9153395]

Hogarty MD. The requirement for evasion of programmed cell death in neuroblastoma with MYCN amplification. Cancer Letter. 2003; 197:173–179.

Horvilleur E, Bauer M, Goldschneider D, Mergui X, de la Motte A, Bénard J, et al. p73alpha isoforms drive opposite transcriptional and post-transcriptional regulation of MYCN expression in neuroblastoma cells. Nucleic Acids Res. 2008; 36:4222–4232. [PubMed: 18583365]

Jones SN, Hancock AR, Vogel H, Donehower LA, Bradley A. Overexpression of Mdm2 in mice reveals a p53-independent role for Mdm2 in tumorigenesis. Proc Natl Acad Sci U S A. 1998; 95:15608–15612. [PubMed: 9861017]

Lai Z, Freedman DA, Levine AJ, McLendon GL. Metal and RNA binding properties of the hdm2 RING finger domain. Biochemistry. 1998; 37:7005–7015. [PubMed: 9836595]

Lazarova DL, Spengler BA, Biedler JL, Ross RA. HuD, a neuronal-specific RNA-binding protein, is a putative regulator of N-myc pre-mRNA processing/stability in malignant human neuroblasts. Oncogene. 1999; 18:2703–2710. [PubMed: 10348344]

Manohar CF, Short ML, Nguyen A, Nguyen NN, Chagnovich D, Yang Q, et al. HuD, a neuronal-specific RNA-binding protein, increases the in vivo stability of MYCN RNA. J Biol Chem. 2002; 277:1967–1973. [PubMed: 11711535]

Matthay KK. MYCN expression in neuroblastoma: A mixed message? J Clin Oncol. 2000; 18:3591–3594. [PubMed: 11054431]

Mayo LD, Donner DB. A phosphatidylinositol 3-kinase/Akt pathway promotes translocation of Mdm2 from the cytoplasm to the nucleus. Proc Natl Acad Sci U S A. 2001; 98:11598–11603. [PubMed: 11504915]

Meek DW, Knippschild U. Posttranslational modification of MDM2. Mol Cancer Res. 2003; 1:1017–1026. [PubMed: 14707285]

Momand J, Zambetti GP, Olson D, George D, Levine AJ. The MDM-2 oncogene product forms a complex with the p53 protein and inhibits p53-mediated transactivation. Cell. 1992; 69:1237–1245. [PubMed: 1535557]

Negroni A, Scarpa S, Romeo A, Ferrari S, Modesti A, Raschella G. Decrease of proliferation rate and induction of differentiation by a MYCN antisense DNA oligomer in a human neuroblastoma cell line. Cell Growth & Diff. 1991; 2:511–518.

Okamoto K, Li H, Jensen MR, Zhang T, Taya Y, Thorgeirsson SS, et al. Cyclin G recruits PP2A to dephosphorylate Mdm2. Mol Cell. 2002; 9:761–971. [PubMed: 11983168]

Peirce SK, Findley HW. The MDM2 antagonist nutlin-3 sensitizes p53-null neuroblastoma cells to doxorubicin via E2F1 and Tap73. Int J Oncol. 2009; 34:1395–1402. [PubMed: 19360352]

Poyurovsky MV, Jacq X, Ma C, Karni-Schmidt O, Parker PJ, Chalfie M, et al. Nucleotide binding by the Mdm2 RING domain facilitates Arf-independent Mdm2 nucleolar localization. Mol Cell. 2003; 12:875–887. [PubMed: 14580339]

Ross RA, Lazarova DL, Manley GT, Smitt PS, Spengler BA, Posner JB, et al. HuD, a neuronal-specific RNA-binding protein, is a potential regulator of MYCN expression in human neuroblastoma cells. Eur J Cancer. 33:2071–2074. [PubMed: 9516855]

Schweigerer L, Breit S, Wenzel A, Tsunamoto K, Ludwig R, Schwab M. Augmented MYCN expression advances the malignant phenotype of human neuroblastoma cells: evidence for induction of autocrine growth factor activity. Cancer Res. 1990; 50:4411–4416. [PubMed: 2364393]

Seeger RC, Brodeur GM, Sather H, Dalton A, Siegel SE, Wong KY, et al. Association of multiple copies of the N-myc oncogene with rapid progression of neuroblastomas. New Engl J Med. 1985; 313:1111–1116. [PubMed: 4047115]

Sivak LE, Tai KF, Smith RS, Dillon PA, Brodeur GM, Carroll WL. Autoregulation of the human N-myc oncogene is disrupted in amplified but not single-copy neuroblastoma cell lines. Oncogene. 1997; 15:1937–1946. [PubMed: 9365240]

Slack A, Chen Z, Tonelli R, Pule M, Hunt L, Pession A, et al. The p53 regulatory gene MDM2 is a direct transcriptional target of MYCN in neuroblastoma. Proc Natl Acad Sci USA. 2005; 102:731–736. [PubMed: 15644444]

Tang XX, Zhao H, Kung B, Kim DY, Hicks SL, Cohn SL, et al. The MYCN enigma: significance of MYCN expression in neuroblastoma. Cancer Res. 2006; 66:2826–2833. [PubMed: 16510605]

Thompson J, Zamboni WC, Cheshire PJ, Lutz L, Luo X, Li Y, et al. Efficacy of systemic administration of irinotecan against neuroblastoma xenografts. Clin Cancer Res. 1997; 3:423–431. [PubMed: 9815701]

Wang X, Hall TM Tanaka. Structural basis for recognition of AU-rich element RNA by the HuD protein. Nat Struct Biol. 2001; 8:141–145. [PubMed: 11175903]

Weiss WA, Aldape K, Mohapatra G, Feuerstein BG, Bishop JM. Targeted expression of MYCN causes neuroblastoma in transgenic mice. EMBO J. 1997; 16:2985–2995. [PubMed: 9214616]

Zhang Z, Zhang R. p53-independent activities of MDM2 and their relevance to cancer therapy. Curr Cancer Drug Targets. 2005; 5:9–20. [PubMed: 15720185]

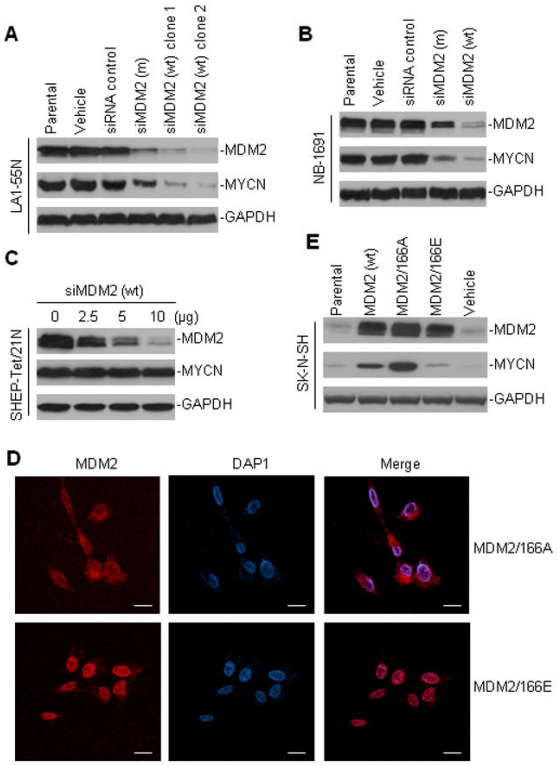

Fig. 1.

Effect of MDM2 modification on MYCN protein expression. **A**, the expression of MDM2 and MYCN in parent LA1-55N cells and LA1-55N transfected with the pSUPER vector only (vehicle), pSUPER containing a control siRNA, a MDM2 siRNA mutant [siMDM2 (m)] and clones transfected with pSUPER/MDM2 wild-type [siMDM2 (wt)] was detected by Western blotting. **B**, NB-1691 cells were transiently transfected with siMDM2 (wt), siMDM2 (m), vehicle and control siRNA, respectively, and expression of MDM2 and MYCN was detected by Western blot assay. **C**, SHEP-Tet/21N cells were transiently transfected with different dose of siMDM2 (wt), and expression of MDM2 and ectopic MYCN was detected by Western blot assay. **D**, subcellular distribution in SK-N-SH cells of transfected MDM2/166A and MDM2/166E, as demonstrated by the red fluorophores seen by confocal microscopy. Scale bars = 10μm. **E**, various forms of MDM2 (wt and mutations 166A or 166E) were stably transfected into SK-N-SH cells, and the expression of transfected MDM2 and endogenous MYCN were detected by Western blot assay.

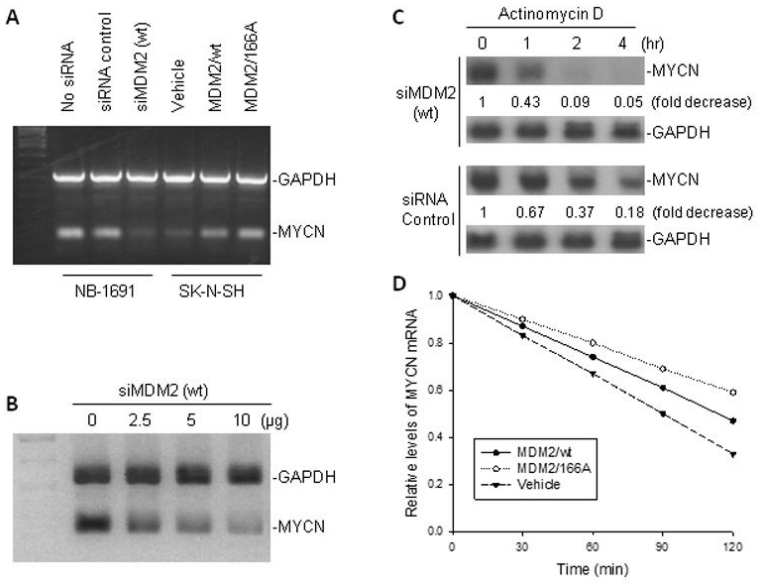

Fig. 2.

Effect of MDM2 modification on MYCN mRNA expression. **A**, RT-PCR results showed the levels of MYCN and GAPDH mRNA expression in NB-1691 cells treated with MDM2 and control siRNA, and in SK-N-SH cells transfected with wt-MDM2 and MDM2/166A plasmids, respectively. **B**, dose-response inhibition of MYCN mRNA by MDM2 siRNA in NB-1691 cells was detected by RT-PCR. **C** and **D**, NB-1691 cells were treated either with MDM2 siRNA or control siRNA (C). SK-N-SH cells were transfected either with wt-MDM2 and MDM2/166A or vehicle control plasmid (D). Cells were then treated with 5mg/ml actinomycin D. At different times after addition of actinomycin D the cells were harvested, and then total RNA was isolated. The amount of MYCN mRNA remaining in NB-1691 was determined by Northern blotting and quantified by densitometric analysis. Labels under bands (C) in the blot represent MYCN mRNA levels after normalization to GAPDH, compared with samples (0, defined as 1 unit). Graphical representation (D) of the relative amount of MYCN mRNA, as detected by quantitative RT-PCR in SK-N-SH cells transfected with plasmids as indicated.

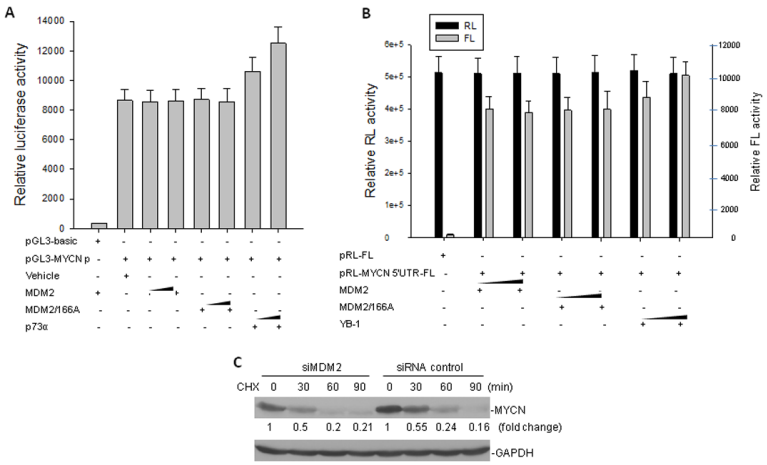

Fig. 3.

Effect of cytoplasmic MDM2 on MYCN transcription, IRES-dependent translation and post-translational regulation. **A**, SK-N-SH cells were co-transfected with 5μg pGL3-MYCN p and with or without increasing amounts (5, 10μg) of MDM2, MDM2/166A and p73α. At 24 hr after transfection, cell extracts were prepared for a luciferase activity assay. **B**, SK-N-SH cells were co-transfected with 5μg pRL-MYCN 5′UTR-FL and increasing amounts (5, 10 μg) of MDM2, MDM2/166A or YB-1 plasmids. RL and FL activities were detected using the Dual-Luciferase Reporter System. **C**, turnover of MYCN protein in LA1-55N cells with or without MDM2 inhibition, as detected by pulse-chase assay. Cells stably transfected with siMDM2 or the control siRNA were treated with cyclohexamide (CHX). At the times indicated post-CHX treatment, cell lysates were prepared for analysis by western blot assay.

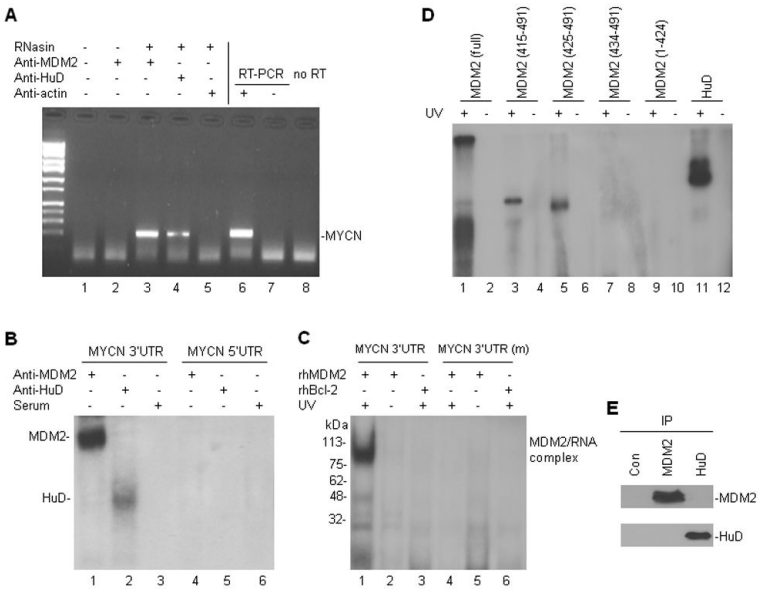

Fig. 4.

MDM2 protein binds to MYCN mRNA *in vivo* and *in vitro*. **A**, cell extracts from SK-N-SH cells transfected with MDM2/166A were prepared in RNA-binding buffer in the presence of RNase inhibitor (RNasin). Following co-IP with anti-MDM2, anti-HuD and anti-actin, the MYCN mRNA was detected by RT-PCR analysis. The positive (NB-1691 total RNA as template, lane 6), the negative (no template, lane 7) and no RT (lane 8) controls for RT-PCR are also shown. **B**, cell extracts from MDM2/166A-transfected SK-N-SH cells were incubated with ^{32}P-labeled RNA probes corresponding to the MYCN 3′UTR and MYCN 5′UTR IRES element, UV cross-linked, and then immunoprecipitated with antibodies as indicated. The protein/RNA probe complexes were run on an SDS-PAGE gel and imaged by autoradiography. **C**, the rhMDM2 and rhBcl-2 were incubated, respectively, with ^{32}P-labeled MYCN 3′UTR and MYCN 3′UTR with AUUUA mutations. The protein/RNA complexes were detected as described in (B). **D**, GST-fused full-length MDM2, different GST-fused MDM2 fragments of the C-terminal RING domain, an MDM2 fragment with a deletion of the C-terminal RING domain and GST-fused HuD were incubated with ^{32}P-labeled MYCN 3′UTR. Formation of MDM2/MYCN RNA complexes was detected as described in (B). **E**, test for a binding interaction between MDM2 and HuD. Cell lysates from NB-1691 were immunoprecipitated (IP) with antibodies as indicated on top. Normal mouse antibody served as a control (Con). Proteins listed on the right that were in the precipitated immune complexes were detected by western blotting.

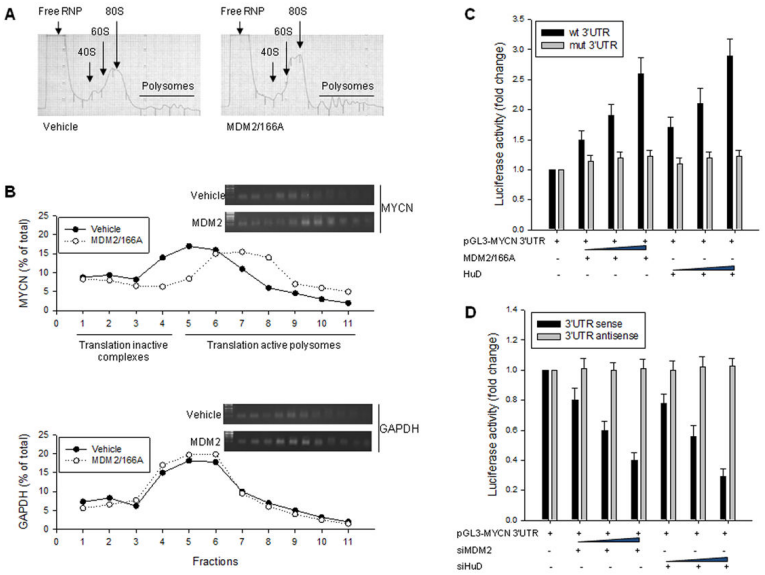

Fig. 5.

MDM2 regulates MYCN translation. **A**, representative polyribosomal profiles from control vector and MDM2/166A transfected SK-N-SH cells. The 254 nm traces obtained during collection of fractions were shown. **B**, relative distributions of MYCN and GAPDH mRNA in SK-N-SH cells transfected either with vehicle or MDM2/166A. The cytoplasmic lysates were fractionated on a sucrose gradient. RNA was extracted from each of the fractions and subjected to quantitative RT-PCR. Data represent percentage of the total amount of corresponding mRNA on each fraction. Relative MYCN and GAPDH mRNA in each fraction obtained by agarose gel electrophoresis are shown (*inserts*). **C**, SK-N-SH cells were co-transfected with 5μg pGL3-MYCN 3′UTR (wt or mutant) plasmids and with increasing amounts (2.5, 5, and 10 μg) of the MDM2/166A or pcDNA 3.1-HuD plasmids. After 24 h, cell extracts were prepared and the quantitative FL (pGL3-MYCN 3′UTR) was detected using the Dual-Luciferase Reporter System. The FL activities in the transfection of pGL3-MYCN 3′UTR only were set at 1. Bars represent the mean ±SD of FL in three independent experiments, normalized to the RL activity. **D**, NB-1691 cells were co-transfected with 5μg pGL3-MYCN 3′UTR (sense or antisense) plasmids and with increasing amounts (2.5, 5, and 10 μg) of the pSUPER-MDM2 or pSUPER-HuD plasmids. Transfection, reporter assays and data presentation were as described in (C).

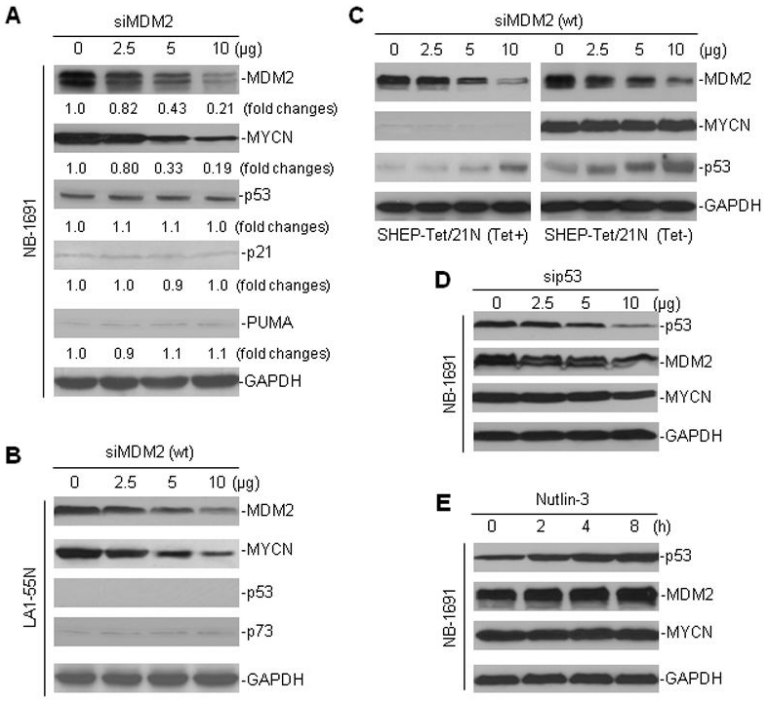

Fig. 6.

MDM2-mediated MYCN expression is p53-independent. **A**, effect of MDM2 inhibition on activation of p53 and its targets in NB-1691. Cells were transfected with different dose of siMDM2 for 24-h, and expression of MDM2, MYCN, p53, p21 and PUMA was detected by Western blot. **B**, Western blot shows the expression of MDM2, MYCN, p53 and p73 in LA1-55N cells treated with siMDM2. **C**, Effect of siMDM2 on regulation of p53 and ectopic MYCN in SHEP-Tet/21N cells in the presence and absence of tetracycline (Tet). Cells were cultured in medium with or without 1 μg/ml Tet and transfected with different amounts of siMDM2 for 24 h. The expression of proteins as indicated was detected by Western blot. **D**, Western blot shows the expression of p53, MDM2 and MYCN in NB-1691 cells treated with sip53 for 24 hours. **E**, Western blot shows the expression of p53, MDM2 and MYCN in NB-1691 treated with 10μM nutlin-3 for the time as indicated.

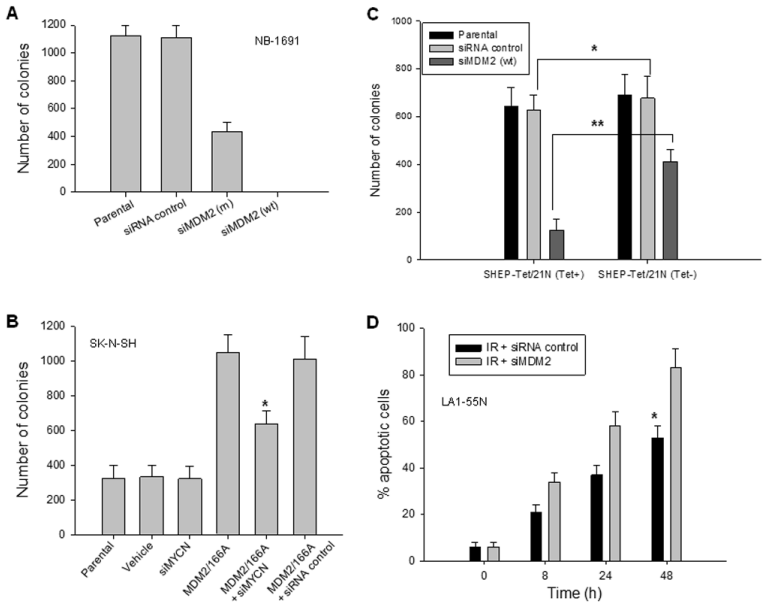

Fig. 7.

Effect of MDM2 modification on MYCN-mediated cell growth in neuroblastoma. **A,** clonogenic assay of NB-1691 cells transfected with siMDM2 (wt) and (m) as well as control siRNA . Cells (1×10^4) were seeded in soft agarose and cultured for 2-3 weeks and then colonies were counted. Data represent the mean of three independent experiments; *bars*, ± SD. **B**, clonogenic assay of SK-N-SH cells that were stably transfected with MDM2/166A plasmid in the presence or absence of siMYCN and control siRNA, **p*<0.01. **C**, comparison of the effect of MDM2 inhibition on growth of cells with and without conditional MYCN expression. SHEP-Tet/21N cells in cultures with or without tetracycline (Tet) were similarly transfected with siMDM2 and control siRNA, and clonogenic assays were performed as in (A), **p*>0.05, ***p*<0.01. **D**, time-course of apoptosis induced by IR in LA1-55N cells in the presence of siMDM2 or siRNA control. The siRNA stably transfected LA1-55N cells were treated with 10 Gy IR for the indicated time points, and apoptotic cells were detected by annexin-V staining using flow cytometry. Data represent the mean percentage of annexin-V positive cells from three independent experiments; *bars*, ± SD. **p*<0.01.